IET Microwaves, Antennas & Propagation

Research Article

IET Journals
The Institution of Engineering and Technology

Composite right/left-handed based compact and high gain leaky-wave antenna using complementary spiral resonator on HMSIW for Ku band applications

ISSN 1751-8725
Received on 29th May 2017
Revised 9th December 2017
Accepted on 2nd February 2018
E-First on 22nd March 2018
doi: 10.1049/iet-map.2017.0478
www.ietdl.org

Anirban Sarkar[1] ✉, Moitreya Adhikary[1], Abhishek Sharma[1], Animesh Biswas[1], Mohammed Jaleel Akhtar[1], Zhirun Hu[2]

[1]Department of Electrical Engineering, Indian Institute of Technology Kanpur, Kanpur, UP-208016, India
[2]School of Electrical and Electronic Engineering, The University of Manchester, Manchester-M139PL, UK
✉ *E-mail: anirban.skr227@gmail.com*

Abstract: In this communication, a novel compact high gain composite right/left-handed (CRLH) based leaky-wave antenna (LWA) is presented at Ku band. A half-mode substrate-integrated waveguide incorporated with a suitably oriented complementary quad spiral resonator (CQSR) is used to achieve a CRLH LWA. The unit cell is realised by a CQSR in such a way that the orientation of spirals exhibits higher leakage loss having a minimum cross coupling between them. The antenna is capable of scanning backward to forward along with a broadside direction in visible space. The proposed configuration has a length of $4.85\lambda_0$ which can scan within the frequency range of 13.5–17.8 GHz having a beam scanning range of 86° (−66° to 20°) and a maximum gain of 16 dBi. The simulated reflection coefficient of the proposed antenna is below −10 dB throughout the working frequency range with a side-lobe level of below −10 dB. The designed prototype is more compact in nature having high gain, fair scanning range, and good cross-polarisation level along with simpler design methodology and tuning capability to enhance the gain as well as radiation efficiency maintaining a fixed size. The proposed antenna could be a promising candidate in Ku-band applications like fixed satellite services, and broadcast satellite services etc.

1 Introduction

Leaky-wave antennas (LWAs) are affiliated to the travelling-wave antenna family based on a transmission line with periodic radiating elements [1]. For the past few decades, numerous LWAs have been reported with the development of various microwave transmission lines (TLs) including rectangular and circular waveguides [2, 3], various planar waveguides like parallel plate waveguides [4], micro-strip lines [5, 6], co-planar waveguides [7], dielectric slabs [8] etc. However, at high frequency it is not feasible to use micro-strip-based LWAs because of high conductor loss and low efficiency. Though the waveguide-based LWAs can be used at higher frequencies the integration with other planar structures is quite difficult. On the other hand, a substrate-integrated waveguide (SIW) is a good compromise between a dielectric filled waveguide and a micro-strip and has become popular in recent years for its significant advantages such as low profile, low cost, light weight, and easy integration [9]. Along with the above advantages, due to its high efficiency, high gain, and narrow elevation beam-width make SIW an attractive candidate for LWA and opens a new avenue for frequency beam scanning application. Several SIW-based LWAs have been reported in [10–13]. Over the last few years, the use of half-mode SIW (HMSIW) in designing LWAs has also increased extensively. It avails all the advantageous features of SIW structures along with the size reduction by a factor of half [14, 15]. However, these suffer from the problem of an open stop-band (OSB) where broadside radiation is null. Therefore, backward-broadside-forward frequency beam scanning is not achieved. To mitigate this problem, several techniques are developed and employed in designing LWA with full-space scanning [16–18]. In [19], a quarter-wave transformer, or alternatively a matching stub is proposed to eliminate the stop-band in designing one-dimensional (1-D) conventional periodic micro-strip LWA at K-band but it suffers from a narrow bandwidth as well as a smaller beam scanning range and this concept is validated experimentally in [20]. Some other techniques are also proposed to eliminate the stop-band, like unit cells are placed in transversal asymmetry [21], lattice-network based TL model [22], using a π-matching network [23] in designing periodic LWAs. In [24], a self-matched periodic LWA is designed in a micro-strip environment using a U-stub and an inter-digital capacitor which is compact in size with a suitable scanning range but has a maximum gain of 10.6 dBi. Recently, several composite right/left-handed (CRLH) based antennas have been reported using a micro-strip, SIW, CRLH rectangular waveguide etc. They own some unique features not available for conventional microwave structures such as it supports both backward and forward waves and this is applicable for LWAs for achieving continuous beam steering in visible space. CRLH based LWAs with a detailed dispersion analysis in a micro-strip environment is reported in [25]. A K-band frequency-scanned LWA based on CRLH TLs is reported in [26]. In [27], the CRLH SIW based LWA with low cross-polarisation level is shown. The CRLH SIW-based LWA with polarisation flexibility is shown in [28]. It is to be noted that the side-wall vias of HMSIW structures provide an effective shunt inductance and hence, to implement the CRLH medium, only series capacitance is required. By utilising these benefits of HMSIW, several CRLH HMSIW based LWAs have been reported in the past [14, 29–31] where full space scanning is achieved by solving the OSB issues for the unbalanced transmission line. However, most of the previously reported antennas are not exhibiting a high gain with significantly decreasing the overall profile of the structure.

Our main aim in this work is to propose a compact low profile LWA having higher gain and improved radiation efficiency which takes advantage of all the characteristics of HMSIW structures. This is facilitated by introducing the novel concept of complementary spiral resonators which help in obtaining better control of design parameters thereby providing easier tuning. The proposed design is also compared with other reported works. To the best of author's knowledge, such a type of CRLH-based LWA with compact size, high gain, improved side lobe level and more flexible in tuning has not been earlier proposed in the literature. The proposed antenna is simulated as well as optimised for Ansoft

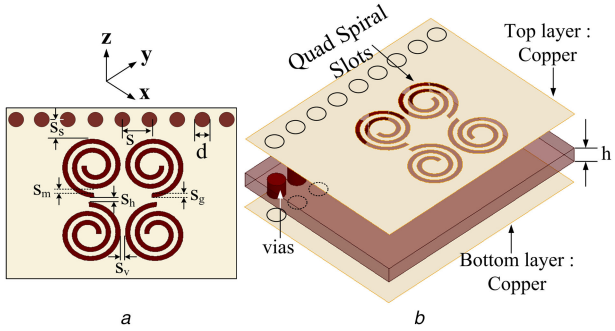

Fig. 1 *Geometry of the proposed CQSR unit cell in HMSIW*
(a) Top view, ***(b)*** 3D view. Geometrical parameters: $S = 1.6$, $d = 0.8$, $S_m = 0.22$, $S_h = 0.24$, $S_v = 0.24$, $S_g = 0.18$, $S_s = 1.23$ (all values are in mm)

high frequency structure simulator (HFSS) and the same is fabricated and tested. Along with the good frequency scanning range and high gain of the proposed prototype, the antenna has advantageous in terms of compactness, a simple single layered fabrication process that can be easily implemented on a printed circuit board.

2 Unit cell design and analysis

2.1 Design of complementary quad spiral resonator (CQSR) unit cell

The top and perspective views of the proposed CQSR unit cell in HMSIW are shown in Fig. 1. The proposed structure is designed on an RT/Duroid 5880 substrate with dielectric constant $(\epsilon_r) = 2.2$, loss tangent $(\tan\delta) = 0.0009$ and height (h) of 0.787 mm. Shunt capacitance and series inductance are distributed along with the geometry, which corresponds to an equivalent model of ground plane and the top wall of the HMSIW structure, respectively. A group of four complementary spiral slots is etched on the top wall of the HMSIW which provide a series capacitance, whereas metallic vias are realised as distributed shunt inductance. Thus, the combined effects support the property of left-handed (LH) region. The length of the unit cell is chosen by maintaining the homogeneity condition, i.e. unit cell length $\ll \lambda_g/4$. By satisfying the balanced condition of the proposed unit cell, backward to forward frequency beam scanning together with broadside radiation is obtained. This implies the elimination of band-gap between LH and right-handed (RH) regions. The balanced condition for the unit cell is established by tuning the values of S_m, S_h, S_v, S_g, S_s at a fixed cut-off frequency and the LH region only gets affected by these parameters. The quad of spirals with suitable orientation is exploited as a unit cell of the proposed antenna in such a manner that radiation loss in terms of normalised leakage constant is enhanced and showing a smooth variation within the desired frequency band. The dependency on a number of spirals on the selection of a unit cell is clearly depicted in Fig. 2*a*, where it is clear that the proposed configuration with four spirals shows most suitable performance among the depicted four cases (in Fig. 2*a*). Though, a similar leakage behaviour is achieved from a unit cell having two spirals but the proposed unit cell is the better selection as the side lobe level is also reduced by ~5.41 dB compared with the unit cell containing two spirals. Moreover, the number of turns of spirals also helps in enhanced leakage loss resulting in improved efficiency and gain. For better understanding, dispersion analysis is done and described next.

2.2 Dispersion analysis

For the better realisation of the behaviour of the LWA, the dispersion characteristic of the CQSR unit cell is studied. It is done through the driven-mode solution which is more time efficient than eigen-mode simulation. In the full wave simulation of the unit cell, wave-port excitation is carried out. By considering the effect of periodicity, the unit cell is simulated in HFSS and the *S*-parameters are extracted to study the dispersion characteristics. During

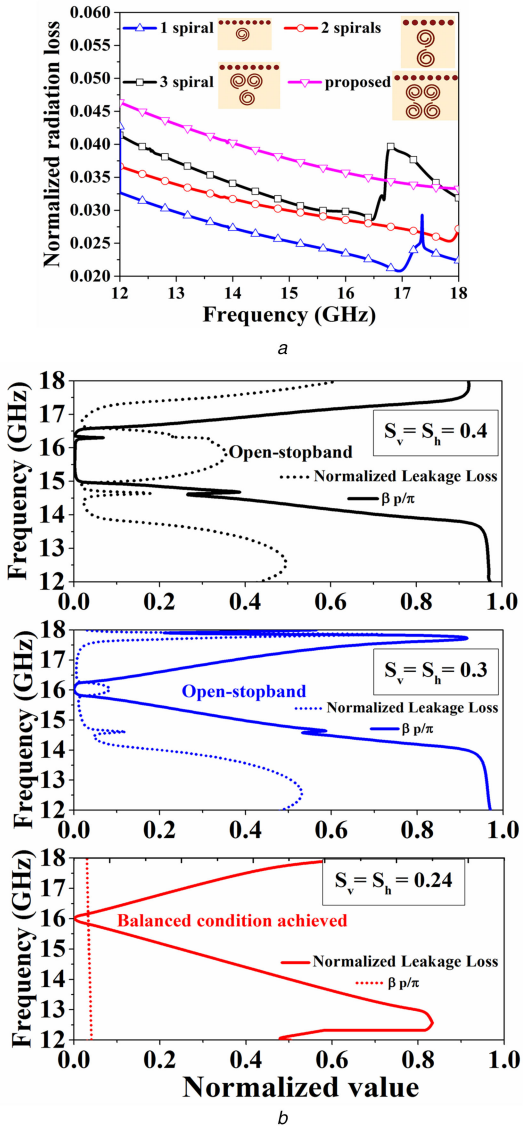

Fig. 2 *Variation of normalised leakage loss for changing*
(a) Number of spirals, ***(b)*** Gap between the spirals with open-stopband elimination

simulation, the mutual coupling effect between the unit cells is neglected. The dispersion equation for the periodic transmission line can be written as [26]

$$\cos(\beta p) = \frac{(A + D)}{2}, \tag{1}$$

where A and D are the components of a transmission matrix of the TL. To extract the dispersion curve from full wave simulation, the equivalent *S*-parameters of the periodic transmission line can be calculated as

$$\beta p = \cos^{-1}\left(\frac{1 - S_{11}S_{22} + S_{12}S_{21}}{2S_{21}}\right), \tag{2}$$

where p is the periodicity of unit cell, β is the propagation constant or radiating space harmonic. In the proposed design, $n = 0$ harmonic is responsible for radiation. For a traditional transmission line, series inductors and shunt capacitors are the distributed elements which exhibit forward wave propagation. The LH transmission line is the dual of the RH TL structure and it exhibits backward-wave propagation. It is observed from Fig. 3*a*, at the transition frequency (16 GHz) of the RH and LH regions, series (ω_{se}) and shunt (ω_{sh}) resonant frequencies are equal. Thus, the balance condition is achieved. At this condition, phase constant β exhibits zero value at the transition frequency (ω_0) as

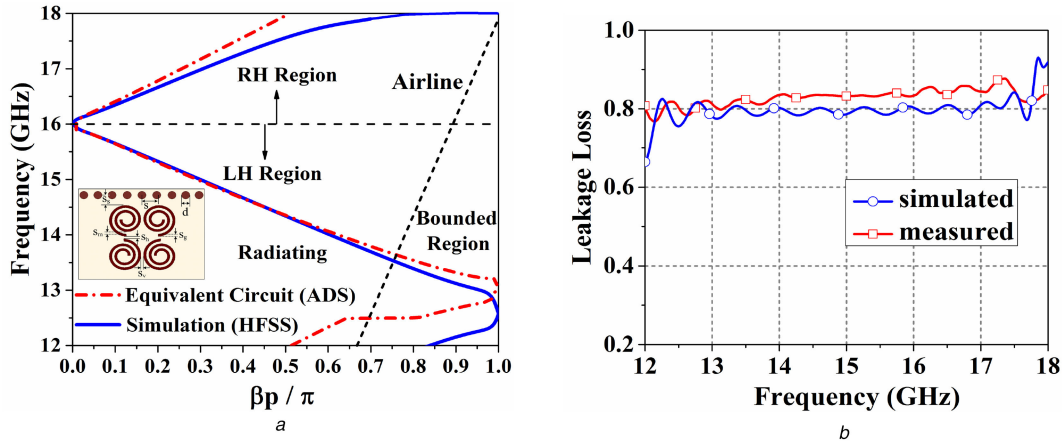

Fig. 3 *Dispersion and leakage loss responses of the proposed unit cell*
(a) Comparison between simulated and optimised dispersion diagram of balanced CQSR unit cell, ***(b)*** Simulated and measured leakage loss

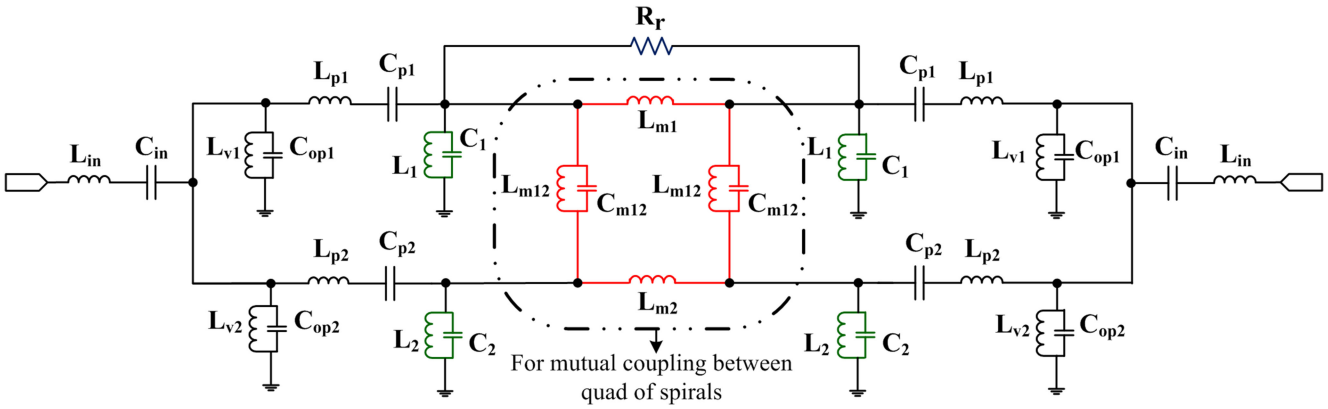

Fig. 4 *Equivalent circuit model of HMSIW CQSR unit cell. Extracted circuit element values are* $L_{in} = 0.367\,nH$, $C_{in} = 0.486\,pF$, $L_{v1} = 2.06\,nH$, $C_{op1} = 0.205\,pF$, $L_{v2} = 0.697\,nH$, $C_{op2} = 0.171\,pF$, $L_{p1} = 2.974\,nH$, $C_{p1} = 2.924\,pF$, $L_{p2} = 1.132\,nH$, $C_{p2} = 0.122\,pF$, $L_1 = 0.482\,nH$, $C_1 = 0.1\,pF$, $L_2 = 0.887\,nH$, $C_2 = 0.942\,pF$, $L_{m1} = 2.99\,nH$, $L_{m2} = 2.97\,nH$, $L_{m12} = 1.905\,nH$, $C_{m12} = 0.452\,pF$, $R_{r=1.416\,ohm}$

$$\omega_0 = \frac{1}{\sqrt[4]{L_R C_R L_L C_L}} = \omega_{se} = \omega_{sh}. \tag{3}$$

Below this frequency, the LH region appears which supports the propagation of backward-wave and just above the transition frequency is the RH region which supports forward-wave. The simulated and measured leakage loss [32] of the unit cell is depicted in Fig. 3*b* where it is clear that the radiation loss has a higher value due to the proposed CQSR unit cell. The radiation from the unit cell in terms of leakage loss is varying with low fluctuation from 0.8 to 0.87 within the working frequency range which is desired for good antenna design. In Fig. 2*b*, the effect of variation on the inter-spiral gap (S_h or S_v) to determine the balance condition is shown where it varies from $S_h = S_v = 0.4$ mm (with an open stop band) to $S_h = S_v = 0.24$ mm (the open stop band is eliminated).

3 Equivalent circuit model

In this proposed LWA, the CRLH structure is realised in HMSIW and the equivalent circuit for the proposed structure is modelled by Advanced Designed System (ADS) software where dispersion characteristic is analysed through optimisation. Primarily, initial values of the equivalent circuit are predicted from *S*-parameter responses of unbalanced unit-cell (HFSS) by fitting the circuit model in ADS. Furthermore, the equivalent model parameters are tuned in ADS to achieve balance condition. The change in circuit element values from the initial prediction gives an insight into the direction of the required changes in physical parameters of the unit cell in HFSS design in order to achieve balanced condition. For example, the change in values of $L_{m12} - C_{m12}$ indicates the corresponding change in physical parameter S_h. Similarly, a change in L_{m1} and L_{m2} can be related to the corresponding change of S_v. The width and turns of the complementary spiral can be modelled by the equivalent circuit elements $L_1 - C_1$ (for spirals close to the via-wall) and $L_2 - C_2$ (for spirals close to the magnetic wall). The detailed and precise equivalent circuit for the proposed HMSIW CQSR unit cell is shown in Fig. 4, where the encircled area of the circuit is showing the effect of mutual coupling between the single quad of complementary spirals, neglecting the diagonal mutual coupling. L_1, C_1, L_2, C_2 are coming for a quad of spirals which are represented by four L–C tank circuits. The parallel inductors (L_{v1} and L_{v2}) and capacitors (C_{op1} and C_{op2}) are obtained due to the metallic vias and considering the fringing field at the magnetic wall, respectively. All the optimised inductors and capacitor values are mentioned in Fig. 4. The comparison between simulated and optimised dispersion characteristics is depicted in Fig. 3*a* and it is showing a good agreement

$$Z_B = Z_L \sqrt{\frac{(\omega/\omega_{se})^2 - 1}{(\omega/\omega_{sh})^2 - 1} - \left(\frac{\omega_L}{2\omega}\left[\left(\frac{\omega}{\omega_{se}}\right)^2 - 1\right]\right)^2}, \tag{4}$$

where

$$Z_L = \sqrt{\frac{L_L}{C_L}}, \quad \omega_{se} = \frac{1}{\sqrt{L_R C_L}}, \quad \omega_{sh} = \frac{1}{\sqrt{L_L C_R}}, \quad \omega_L = \frac{1}{\sqrt{L_L C_L}}, \tag{5}$$

$$Z_B = \pm Z_0 \sqrt{\frac{(1 + S_{11})^2 - S_{21}^2}{(1 - S_{11})^2 - S_{21}^2}}. \tag{6}$$

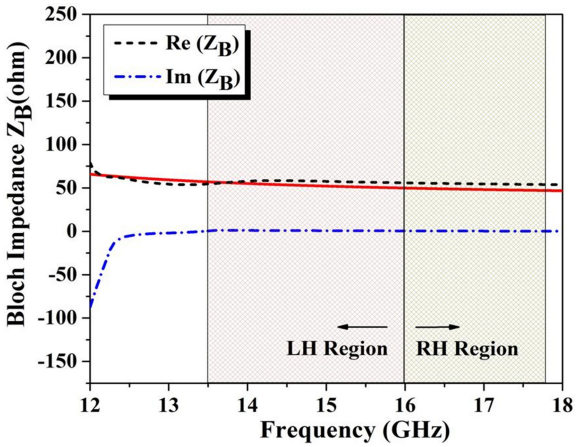

Fig. 5 *Real and imaginary parts of Bloch impedance $Z_B\Omega$ for the proposed structure as a function of frequency. Red line is the impedance at the port of unit cell*

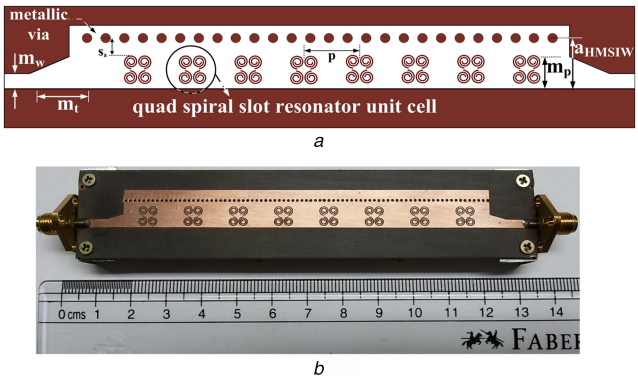

Fig. 6 *Microstrip line fed proposed HMSIW based CRLH CQSR LWA with tapered microstrip transition. Parameter values are: $a_{HMSIW} = 7.47\,mm$, $m_p = 3.61\,mm$, $m_t = 4.35\,mm$, $m_w = 2.29\,mm$, $S_a = 1.6\,mm$, $p = 12\,mm$*
(a) Layout of the proposed antenna, ***(b)*** Fabricated prototype with eight unit cells

The *Bloch* wave analysis can be performed through full wave analysis by considering an infinitely long structure. Here, *Bloch* impedance is extracted from N number of CRLH unit cells, i.e. by a finite unit cell approach as in [33, 34] and is shown in Fig. 5. Mutual coupling is taken into account during analysis. By neglecting the radiation resistance, the *Bloch* impedance Z_B for the symmetric CRLH unit cell is expressed in [32, 33] and mentioned in (4)–(6). From Fig. 5 it is clear that the real part of the *Bloch* impedance is almost matched with the characteristic impedance Z_0 of the transmission line within the desired frequency range (LH and RH regions are depicted shaded in the figure) of the proposed antenna. In that region, the reactive part of Bloch impedance is almost zero, signifying good matching throughout the working frequency region of the antenna.

4 LWA design

Periodic LWAs are generally realised by incorporating periodic perturbations to the guided mode of the structure such that $n = 0$ becomes radiating harmonic in nature. The unit cell shown in Fig. 1 is placed periodically in series with the periodicity p (maintaining the homogeneity condition, i.e. $p \ll \lambda_g/4$) in such a manner that the scanning range of the LWA will be in the fast wave region (13.5–17.8 GHz) where nth space harmonic phase constant (β_n) increases from negative ($\beta_n = -k_0$) to positive ($\beta_n = k_0$) values with increment of frequencies. Moreover, the average cell size p must be substantially smaller than the guided wavelength λ_g to satisfy the homogeneity condition. In the fast wave region, β_n is less than the free space wave number, i.e. $|\beta_n| < k_0$ which is necessary radiation condition of LWA. Fig. 6*a* depicts the layout of the proposed LWA having eight unit cells. To match the structure

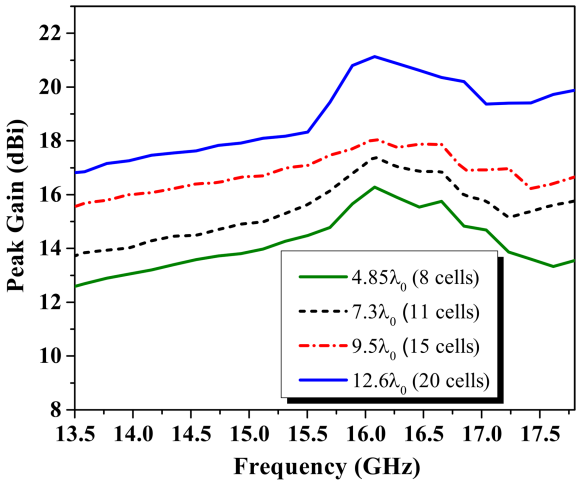

Fig. 7 *Variation of simulated gain with frequencies for different lengths*

with the 50 Ω micro-strip line, taper-line transitions are used at both ends. The m_t and m_p are optimised for the purpose of good matching. The phase constant of the nth spatial harmonic β_n determines the direction of the radiated main beam measured from the broadside direction to both sides of the visible space. The angle of the maximum radiated beam direction (θ_m) can be calculated in dominant mode $n = 0$ as [18]

$$\theta_m = \sin^{-1}\left(\frac{\beta_n}{k_0}\right) = \sin^{-1}\left(\frac{\beta_0}{k_0} + \frac{n\lambda_0}{p}\right). \quad (7)$$

Equation (7) shows that a full space scanning (-90° to 90°) can be achieved if β_n varies with the range ($-k_0$, k_0). Fig. 7 shows the variation of a simulated peak gain with frequencies for different radiator lengths where the gain is increasing with radiator length and is maximum at broadside. The proposed antenna stands as a very good candidate in terms of compactness, frequency scanning range and gains for the applications in this frequency range.

5 Experimental verification and discussion

The proposed HMSIW CRLH CQSR based LWAs are fabricated on a Rogers RT/Duroid 5880 substrate having a dielectric constant of 2.2, loss tangent ($\tan\delta$) of 0.0009 and thickness of 0.787 mm shown in Fig. 6*b*. The overall dimension of the proposed antenna (including feeding network) is $121.5 \times 24.5 \times 0.787\ mm^3$ ($4.85\lambda_0$ long) which is much more compact than other reported designs with the promising property of a broadband scanning range at Ku-band. Fig. 8 shows the simulated and measured S-parameters of the proposed antenna which exhibits an impedance bandwidth of 27.47% (simulated) and 25.80% (measured) within the radiating fast wave region. The pass-band before 13.5 GHz signifies the bounded wave propagation and there is a stop-band beyond 17.8 GHz. Fig. 9 shows the comparison between simulated and measured normalised H-plane (y–z plane) radiation patterns with frequencies where all of the beam patterns reveal the property of balanced CRLH LWAs, backward to forward continuous frequency beam scanning. In Fig. 8, the radiation patterns at 13.5–15 GHz correspond to the LH radiation regions, 16 GHz corresponds to broadside radiation and up to 17.8 GHz correspond to RH radiation regions. By changing the periodicity p, the transitional frequency of broadside radiation can be tuned keeping a fair scanning range on both sides from the broadside direction. Thus, the scanning range can be modified in the RH region due to increase in positive angles. The measured minimum cross-polarisation levels are achieved as −20.04 dB at 13.5 GHz, −26.89 dB at 14 GHz, −29.26 dB at 14.5 GHz, −19.82 dB at 15 GHz, −25.45 dB at 16 GHz and −23.05 dB at 17.8 GHz for the radiated main beam directions of -66°, -43°, -30°, -17°, 0° and 20°, respectively. The three-dimensional (3-D) radiation pattern of the proposed antenna is shown in Fig. 10 where the radiated fan beam is scanning with the

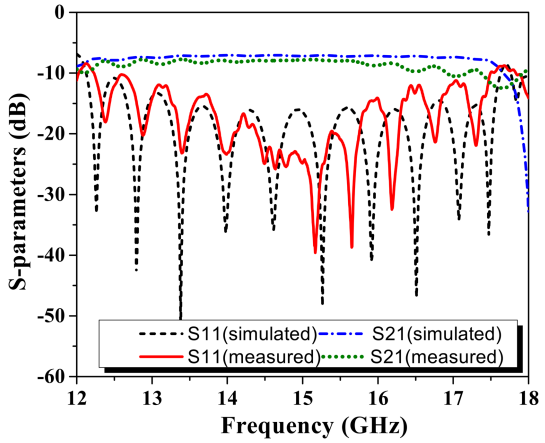

Fig. 8 *Comparison of simulated and measured S-parameters with frequency*

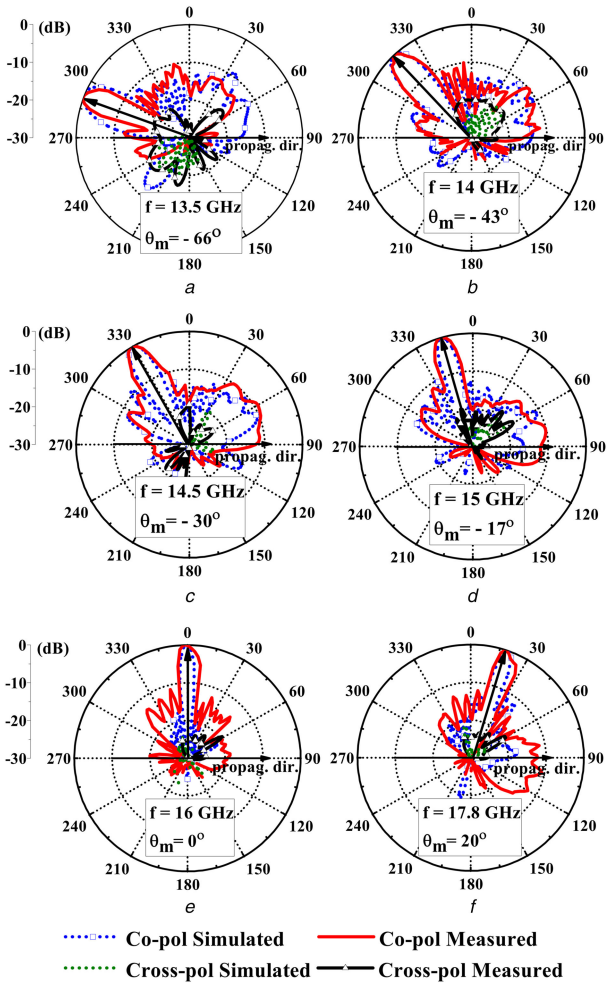

Fig. 9 *Comparison of simulated and measured normalised H-plane (y-z plane) radiation patterns at*
(a) 13.5 GHz, ***(b)*** 14 GHz, ***(c)*** 14.5 GHz, ***(d)*** 15 GHz, ***(e)*** 16 GHz, ***(f)*** 17.8 GHz

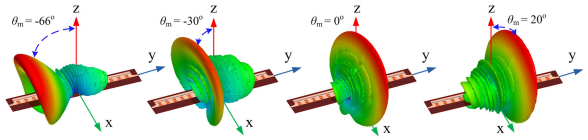

Fig. 10 *3-D fan-beam radiation patterns at 13.5, 14.5, 16 and 17.8 GHz of the antenna*

range of 86° in visible space (y–z plane) with frequencies. Variations of measured peak gain and simulated radiation efficiency with frequencies of the above-mentioned antenna are

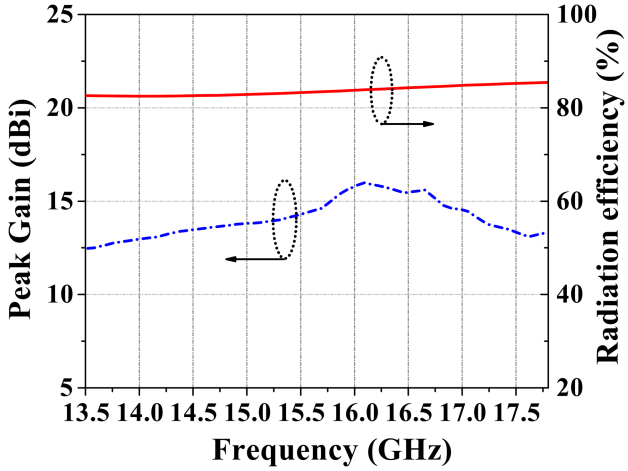

Fig. 11 *Variation of measured peak gain and simulated radiation efficiency as a function of frequency for the proposed structure of* $4.85\lambda_0$

Table 1 Comparison with other reported designs

Ref.	Radiator length	Bandwidth, GHz	Scanning range	Peak gain, dBi
[19]	$22.82\lambda_0$	26–27.5 (5.6%)	10°	16
[20]	$11.57\lambda_0$	8–11.4 (35.05%)	35°	21
[24]	$7.44\lambda_0$	5–7 (33.33%)	155°	10.6
[26]	$12.95\lambda_0$	20–30 (40%)	75°	14
[27]	$5.74\lambda_0$	13.5–17.8 (27.47%)	87°	9.4
[30]	$6.6\lambda_0$	8.4–11.4 (30.3%)	86°	11
[32]	$5.67\lambda_0$	8.6–10.3 (17.98%)	86°	11.5
this work	$4.85\lambda_0$	13.5–17.8 (27.47%)	86°	16

λ_0: Wavelength at the centre frequency.

shown in Fig. 11. The measured antenna gain varies from 12–16 dBi and the estimated radiation efficiency [25] is varied from 82 to 85% within the desired frequency range. The proposed antenna is advantageous in terms of compactness and gain with good scanning angle capabilities than other reported designs that concluded in Table 1.

6 Conclusion

A compact frequency beam scanning high gain CQSR-based (balanced CRLH) HMSIW LWA is presented at Ku band. Matched balanced condition is achieved for the unit cell. Thus the proposed geometry is able to scan from backward to forward including broadside direction within a wide frequency range of 13.5–17.8 GHz with a scanning range of 86° (−66° to 20°) maximum simulated and measured gain of 16.28 and 16 dBi, respectively. The simpler and compact design methodology along with easier tuning capability for further enhancing gain and radiation efficiency make this proposed antenna as an appealing candidate for many practical applications in Ku-band like fixed satellite services, broadcast satellite services.

7 Acknowledgments

The authors would like to thank Dr Arun K. Bhattacharyya, Northrop Grumman Systems Corporation for his valuable suggestions.

8 References

[1] Jackson, D.R., Oliner, A.A.: 'Leaky-wave antennas', in Balanis, C.A. (Ed.): '*Modern antenna handbook*' (Wiley, Hoboken, NJ, USA, 2008), pp. 325–367
[2] Goldstone, L.O., Oliner, A.A.: 'Leaky-wave antennas I: rectangular waveguides', *IEEE Trans. Antennas Propag.*, 1959, **7**, (10), pp. 307–319
[3] Goldstone, L.O., Oliner, A.A.: 'Leaky-wave antennas II: circular waveguides', *IEEE Trans. Antennas Propag.*, 1961, **9**, (3), pp. 280–290

[4] Lee, U.H.C.J.I., Cho, Y.K.: 'Analysis for a dielectric filled parallel plate waveguide with finite number of periodic slots in its upper wall as a leaky-wave antenna', *IEEE Trans. Antennas Propag.*, 1999, **47**, (4), pp. 701–706
[5] Menzel, W.: 'A new traveling wave antenna in microstrip'. Proc. 8th IEEE European Microwave Conf., 1978, pp. 302–306
[6] Liu, J., Long, Y.: 'Analysis of a microstrip leaky-wave antenna loaded with shorted stubs', *IEEE Antennas Wirel. Propag. Lett.*, 2008, **7**, pp. 501–504
[7] Grbic, A., Eleftheriades, G.V.: 'Leaky CPW-based slot antenna arrays for millimeter wave applications', *IEEE Trans. Antennas Propag.*, 2002, **50**, (11), pp. 1494–1504
[8] Schwering, F.K., Peng, S.T.: 'Design of dielectric grating antennas for millimeter wave applications', *IEEE Trans. Microw. Theory Tech.*, 1983, **31**, (2), pp. 199–209
[9] Deslandes, D., Wu, K.: 'Single-substrate integration technique of planar circuits and waveguide filters', *IEEE Trans. Antennas Propag.*, 2003, **51**, (2), pp. 593–596
[10] Deslandes, D., Wu, K.: 'Substrate integrated waveguide leaky-wave antenna: concept and design considerations'. IEEE Asia–Pacific Microwave Conf., Suzhou, China, 2005
[11] Liu, J., Tang, X., Li, Y.*, et al.*: 'Substrate integrated waveguide leaky-wave antenna with H-shaped slots', *IEEE Trans. Antennas Propag.*, 2012, **60**, (8), pp. 3962–3967
[12] Liu, J., Jackson, D., Long, Y.: 'Substrate integrated waveguide (SIW) leaky-wave antenna with transverse slots', *IEEE Trans. Antennas Propag.*, 2012, **60**, (1), pp. 20–29
[13] Mohtashami, Y., Rashed-Mohassel, J.: 'A butterfly substrate integrated waveguide leaky-wave antenna', *IEEE Trans. Antennas Propag.*, 2014, **62**, (6), pp. 3384–3388
[14] Xu, J., Hong, W., Tang, H.*, et al.*: 'Half-mode substrate integrated waveguide (HMSIW) leaky-wave antenna for millimeterwave applications', *IEEE Antennas Wirel. Propag. Lett.*, 2008, **7**, pp. 85–88
[15] Saghati, A.P., Mirsalehi, M.M., Neshati, M.H.: 'A HMSIW circularly polarized leaky-wave antenna with backward, broadside, and forward radiation', *IEEE Antennas Wirel. Propag. Lett.*, 2014, **13**, pp. 451–454
[16] Caloz, C., Itoh, T.: '*Electromagnetic metamaterials: transmission line theory and microwave applications*' (Wiley/IEEE, Hoboken, NJ, 2005)
[17] Liu, L., Caloz, C., Itoh, T.: 'Dominant mode leaky-wave antenna with backfire-to-endfire scanning capability', *Electron. Lett.*, 2002, **38**, (23), pp. 1414–1416
[18] Caloz, C., Jackson, D.R., Itoh, T.: 'Leaky-wave antennas', in Gross, F.B. (Ed.): '*Frontiers in antennas*' (McGraw-Hill, New York, NY, USA, 2011), pp. 339–409
[19] Paulotto, S., Baccarelli, P., Frezza, F.*, et al.*: 'A novel technique for open-stopband suppression in 1-D periodic printed leakywave antennas', *IEEE Trans. Antennas Propag.*, 2009, **57**, (7), pp. 1894–1906
[20] Williams, J.T., Baccarelli, P., Paulotto, S.*, et al.*: '1-D combline leaky-wave antenna with the open-stopband suppressed: design considerations and comparisons with measurements', *IEEE Trans. Antennas Propag.*, 2013, **61**, (9), pp. 4484–4492
[21] Otto, S., Al-Bassam, A., Rennings, A.*, et al.*: 'Transversal asymmetry in periodic leaky-wave antennas for Bloch impedance and radiation efficiency equalization through broadside', *IEEE Trans. Antennas Propag.*, 2014, **62**, (10), pp. 5037–5054
[22] Otto, S., Rennings, A., Solbach, K.*, et al.*: 'Transmission line modeling and asymptotic formulas for periodic leaky-wave antennas scanning through broadside', *IEEE Trans. Antennas Propag.*, 2011, **59**, (10), pp. 3695–3709
[23] Baccarelli, P., Paulotto, S., Jackson, D.R.: 'A pi matching network to eliminate the open-stopband in 1-D periodic leaky-wave antennas'. Proc. 2012 IEEE Int. Symp. on Antennas and Propagation, Chicago, IL, July 2012, pp. 1–2
[24] Paulotto, S., Baccarelli, P., Jackson, D.R.: 'A self-matched wide scanning U-stub microstrip periodic leaky-wave antenna', *J. Electromagn. Wave*, 2014, **28**, (2), pp. 151–164
[25] Paulotto, S., Baccarelli, P., Frezza, F.*, et al.*: 'Full-wave modal dispersion analysis and broadside optimization for a class of microstrip CRLH leaky-wave antennas', *IEEE Trans. Microw. Theory Tech.*, 2008, **56**, (12), pp. 2826–2837
[26] Jiang, W., Liu, C., Zhang, B.*, et al.*: 'K-band frequency-scanned leaky-wave antenna based on composite right/left-handed transmission lines', *IEEE Antennas Wirel. Propag. Lett.*, 2013, **12**, pp. 1133–1136
[27] Zhang, H., Jiao, Y.C., Zhao, G.*, et al.*: 'CRLH-SIW-based leaky wave antenna with low cross-polarisation for Ku-band applications', *Electron. Lett.*, 2016, **52**, (17), pp. 1426–1428
[28] Dong, Y., Itoh, T.: 'Substrate integrated composite right-/left-handed leaky-wave structure for polarization-flexible antenna application', *IEEE Trans. Antennas Propag.*, 2012, **60**, (2), pp. 760–771
[29] Dong, Y., Itoh, T.: 'Composite right/left-handed substrate integrated waveguide and half mode substrate integrated waveguide leaky-wave structures', *IEEE Trans. Antennas Propag.*, 2011, **59**, (3), pp. 767–775
[30] Henry, R., Okoniewski, M.: 'A broadside-scanning half-mode substrate integrated waveguide periodic leaky-wave antenna', *IEEE Antennas Wirel. Propag. Lett.*, 2014, **13**, pp. 1429–1432
[31] Oliner, A., Jackson, D.R.: '*Antenna engineering handbook*' (McGraw-Hill, New York, NY, USA, 1993), ch. 11
[32] Yang, Q., Zhao, X., Zhang, Y.: 'Composite right/left-handed ridge substrate integrated waveguide slot array antennas', *IEEE Trans. Antennas Propag.*, 2014, **62**, (4), pp. 2311–2316
[33] Collin, R.: '*Foundations for microwave engineering*' (McGraw-Hill, New York, NY, USA, 1992, 2nd edn.), ch. 8
[34] Suntives, A., Hum, S.V.: 'An electronically tunable half-mode substrate integrated waveguide leaky-wave antenna'. Proc. 5th European Conf. on Antennas and Propagation (EUCAP), April 2011, pp. 3670–3674